# Characterizing Tumor Heterogeneity and Cell Diversity Across Multiple Cancer Types

Leiam Colbert[1], Ben Patterson[1], Cheng-Yi Chen[1], Nicolas Fernandez[1], Jiang He[1]
[1]Vizgen™, 61 Moulton St, Cambridge, Massachusetts, United States

vizgen

## Introduction

For oncologists, the spatial information embedded in the heterogeneous tumor microenvironment plays a critical role in assessing patient prognosis. Vizgen's MERSCOPE™ Platform, built on multiplexed error-robust fluorescence in *situ* hybridization (MERFISH) technology, enables the direct profiling of the spatial organization of patient tumors with sub-cellular resolution, filling an important gap in previous iterations of transcriptomic evaluation. Here, we present a pan-cancer approach using a 500-gene panel to characterize various cancers in human clinical samples using the MERSCOPE™ Platform. **We demonstrate MERSCOPE's ability to spatially profile gene expression across multiple tumor types, including breast, colon, prostate, ovarian, lung, and liver cancer**. Comparisons between experiments across multiple cancer types in fresh-frozen and FFPE preservation formats demonstrated the robustness and reproducibility of this technology. To deeply assess how individual cell types in each tumor are dysregulated by cancer, we compared differentially expressed genes as detected by the MERFISH panel from normal and cancerous liver samples. We identified dysregulation in the *WNT*, *NOTCH*, and *TGFB* signaling pathways in our hepatocellular carcinoma samples; all three of these pathways and crosstalk between the pathways have been described as driving carcinogenesis in hepatocellular carcinoma. **These results demonstrate the power of the MERSCOPE™ Platform to generate individualized, accurate cell atlases from patient-derived tumors and to enable further insights into the relationship between genomic profiles, dysregulated pathways, and disease phenotype**. Such network-centric approaches are critical for assisting with identifying genotypic causes of diseases, classifying disease subtypes, and identifying drug targets.*

**RUO only, not approved for diagnostic or therapeutic purposes*

## Materials and Methods

MERFISH enables the simultaneous measurement of the expression of hundreds of genes, giving insight into the quantity and distribution of RNA transcripts across a tissue slice. Target RNA species are labeled by tiling oligo probes to barcode each transcript in its native 3-dimensional cellular context. Each barcode is fluorescently detected in sequential rounds of imaging to resolve different RNA species (Figure 1)[1].

We designed a MERSCOPE Gene Panel targeting 500 pan-cancer genes including canonical signaling pathways of cancer, cancer type-specific genes, key immune genes, proto-oncogenes, and tumor-suppressor genes for use in several cancer types. The MERSCOPE FF and FFPE Sample Preparation Kits were used along with the MERSCOPE Cell Boundary Staining Kit to utilize segment cells for analysis of cell-cell interactions. Fresh frozen (FF) and FFPE tissues were evaluated from the following human sample types: Normal Liver, Liver Cancer, Breast Cancer, Colon Cancer, Ovarian Cancer, Prostate Cancer, and Lung Cancer.

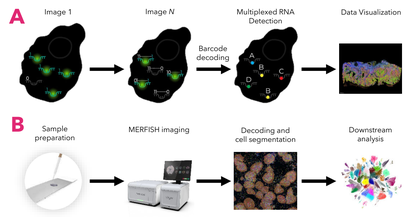


**FIGURE 1. MERFISH process and study design.** (A) During MERFISH, target RNA species are labeled by tiling oligo probes containing different barcodes; each barcode is fluorescently detected in sequential rounds of imaging to resolve the spatial location of different RNA species. (B) Prepared tissue samples were run on the MERSCOPE Instrument for automated MERFISH imaging decoding and cell segmentation before downstream analysis.

## Results

### Concordance between replicates and across preservation methods

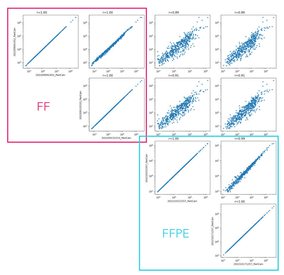


**TABLE 1. Concordance values by sample type.**

| Sample Type | FF correlation | FFPE correlation | FF/FFPE correlation |
|---|---|---|---|
| Breast Cancer | 0.99 | 0.99 | 0.76 |
| Colon Cancer^ | 1.00 | 0.99 | 0.90 |
| Lung Cancer^ | 0.99 | 0.99 | 0.72 |
| Ovarian Cancer | 0.99 | 0.99 | 0.79 |
| Prostate Cancer | 0.94 | 1.00 | 0.83 |
| Liver Cancer | 0.99 | N/A | N/A |
| Normal Liver | 0.99 | N/A | N/A |
| ^ matched | | | |

**FIGURE 2. High concordance between replicates and sample preservation methods in colon cancer tissue.** MERFISH data from matched colon cancer tissue sections show high correlation between FF samples (red box) and FFPE samples (blue box). FF and FFPE samples show relatively high correlation to each other (unboxed graphs, averages reported in Table 1). Concordance with RNA-seq data from each sample type were also calculated, data not shown. Reference data comparing MERFISH to RNA-seq and sc-RNA-seq in mouse brain and liver have been published[2].

### References

1. Spatially resolved, highly multiplexed RNA profiling in single cells (2015). DOI: 10.1126/science.aaa6090
2. Concordance of MERFISH spatial transcriptomics with bulk and single-cell RNA sequencing. DOI: 10.26508/lsa.202201701.
3. The STRING database in 2021: customizable protein-protein networks, and functional characterization of user-uploaded gene/measurement sets. DOI: 10.1093/nar/gkaa1074.
4. The Carcinogenic Role of the Notch Signaling Pathway in the Development of Hepatocellular Carcinoma. DOI: 10.7150/jca.26847.
5. Transforming growth factor-β as a therapeutic target in hepatocellular carcinoma. DOI: 10.1158/0008-5472.
6. Aberrant regulation of Wnt signaling in hepatocellular carcinoma. DOI: 10.3748/wjg.v22.i33.7486.



### Probing gene expression in fresh frozen normal and liver cancer tissue

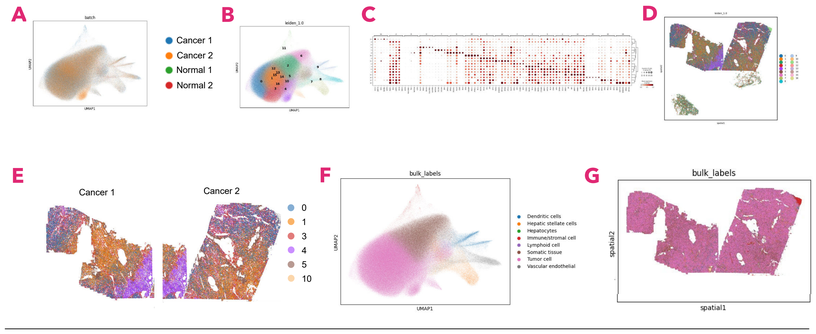


**FIGURE 3. MERFISH analysis of fresh frozen normal liver and liver cancer tissue.** MERFISH experiments with the cancer-specific gene panel were run on 1 normal liver and 1 liver tumor tissue (2 adjacent tissue section replicates each). (A) UMAP of normal and liver cancer tissues shows excellent overlap between samples, indicating sample reproducibility. (B) UMAP with identified clusters (represented by different colors) revealed from unsupervised clustering analysis of MERFISH data. (C) Dot plot illustrating expression of top marker genes across different cell clusters. (D) Spatial map of cell clusters in normal (top) and tumor (bottom) tissues. (E) Tumor cell clusters display a spatial gradient as illustrated by both liver cancer tissue sections. (F) Established marker genes were used to group cell clusters into major cell populations. (G) Cell populations mapped spatially on liver samples.

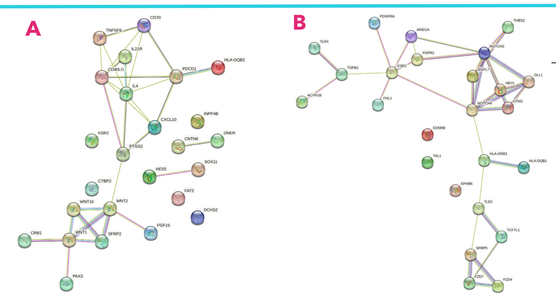


**FIGURE 4. MERFISH data provide insights into gene expression of liver cancer samples.** Gene networks of the top 25 differentially expressed genes in (A) normal sample cells and (B) cancer sample cells.

Our cancer panel can deeply probe genetic expression, allowing us insight into the potential driving mechanisms of these liver cancer samples, namely a dysregulation of *WNT*, *TGFB*, and *NOTCH* signaling (Figure 3C). The high differential expression between normal and tumor tissue highlights the potential use of this panel. Utilizing *STRING-DB*[3] to probe protein association networks in both sample types, we see upregulation for canonical *WNT* signaling and *TNF* activity only enriched in the normal samples (Figure 4A). We again see an enrichment of *WNT*/*TGFB*/*NOTCH* in the cancer sample (Figure B). We observe evidence for dysregulation of 3 major canonical drivers of hepatocellular carcinoma in our cancer samples and asses the complex biology occurring in the cancer interface in a spatially-informed way. Such direct results strongly demonstrate the MERSCOPE's ability to unravel complex tumor biology[4,5,6].

### High reproducibility in fresh frozen colon cancer tissue

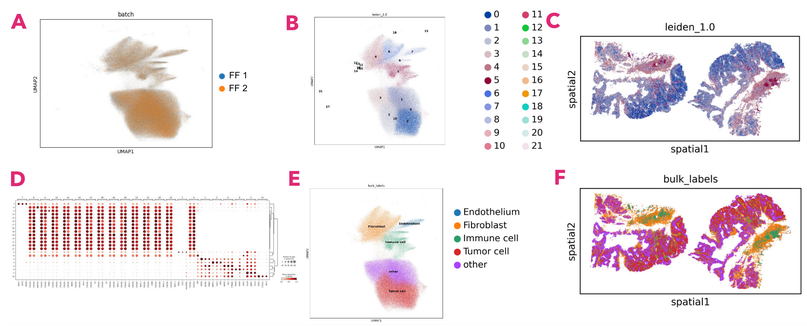


**FIGURE 5. MERFISH identifies molecularly distinct cell types in fresh frozen colon cancer tissue.** (A) UMAP of FF colon cancer tissues shows excellent overlap between samples. (B) UMAP with identified clusters (represented by different colors) revealed from unsupervised clustering analysis of MERFISH data. (C) Spatial mapping shows consistent cluster composition between samples. (D) Dot plot illustrating expression of top marker genes across different cell clusters. (E) Established marker genes were used to group cell clusters into major cell populations. (F) Cell type composition is similar in each tissue slice.

### High reproducibility in FFPE colon cancer tissue

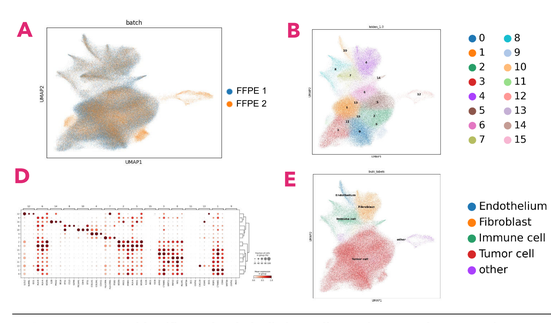


**FIGURE 6. MERFISH identifies molecularly distinct cell types in FFPE colon cancer tissue.** (A) UMAP of FFPE colon cancer tissues shows good overlap between samples. (B) UMAP with identified clusters (represented by different colors) revealed from unsupervised clustering analysis of MERFISH data. (C) Spatial mapping shows consistent cluster composition between samples. (D) Dot plot illustrating expression of top marker genes across different cell clusters. (E) Established marker genes were used to group cell clusters into major cell populations. (F) Cell type composition is similar in each tissue slice.

### High reproducibility in FF and FFPE prostate cancer samples

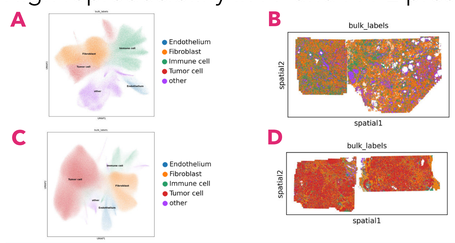


**FIGURE 7. Identification of molecular distinct cell types and their spatial distribution in prostate cancer tissue.** (A) Unsupervised clusters were refined using established marker genes to group cell clusters into major cell populations for fresh frozen (A) and FFPE (C) prostate cancer samples. Cell type composition of fresh frozen (B) and FFPE (D) samples show cell types are reproducible within and between sample types.

### In lung cancer, FF samples correlate while FFPE samples diverge

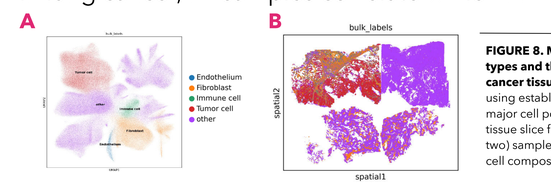


**FIGURE 8. MERFISH identifies molecularly distinct cell types and their spatial distribution in matched lung cancer tissue.** (A) Unsupervised clusters were further refined using established marker genes to group cell clusters into major cell populations. (B) Cell type composition of each tissue slice further illustrate the reproducibility of FF (bottom two) samples, while FFPE (top two) samples have different cell compositions.

### In breast cancer tissue, FF and FFPE samples are similar

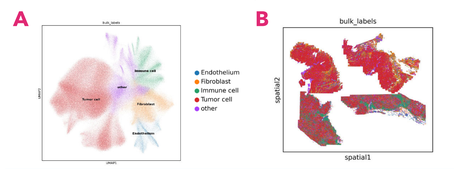


**FIGURE 9. Identification of molecularly distinct cell types and their spatial distribution in breast cancer tissue.** (A) Unsupervised clusters were further refined using established marker genes to group cell clusters into major cell populations. (B) Cell type composition of each tissue slice, cell types are reproducible within and between sample types.

### High reproducibility in FF and FFPE ovarian cancer tissues

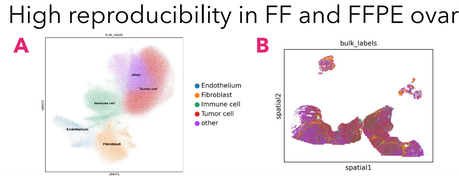


**FIGURE 10. Cell type identification and spatial distribution analysis in ovarian cancer tissue.** (A) Unsupervised clusters were further refined using established marker genes to group cell clusters into major cell populations. (B) Cell type composition of each tissue slice, cell types are reproducible within and between sample types.

## Conclusions

1. We designed a broadly applicable pan-cancer MERFISH gene panel that was used to spatially profile several types of cancer using the MERSCOPE™ Platform.
2. MERSCOPE can reliably detect transcripts in both fresh-frozen and FFPE-preserved tissue types. MERFISH measurements from FF and FFPE tissue blocks often correlate, regardless of whether they are matched samples. Comparing only matched samples may result in higher concordance between samples in future studies.
3. MERFISH Spatial transcriptomic data from MERSCOPE can be used to generate detailed 3-dimensional maps with sufficient resolution to detect morphological features specific to different tissues types.
4. The same pan-cancer MERFISH gene panel robustly detected target genes in 6 major tumor types.
5. MERSCOPE reproducibly detects transcripts in both normal tissues and cancer samples.
6. We identified 3 major canonical drivers of hepatocellular carcinoma in our cancer samples demonstrating the ability of MERFISH data generated by MERSCOPE to unravel complex tumor biology.